

## Research Article

# 3D printing of PCL/Fluorouracil tablets by selective laser sintering: Properties of implantable drug delivery for cartilage cancer treatment

Salmoria GV<sup>1,2\*</sup>, Vieira FE<sup>1</sup>, Ghizoni GB<sup>1</sup>, Marques MS<sup>3</sup> and Kanis LA<sup>3</sup><sup>1</sup>NIMMA, Department of Mechanical Engineering, Federal University of Santa Catarina, 88040-900 Florianópolis, SC, Brazil<sup>2</sup>Biomechanics Engineering Laboratory, University Hospital (HU), Federal University of Santa Catarina, 88040-900 Florianópolis, SC, Brazil<sup>3</sup>Grupo de Desenvolvimento em Tecnologia Farmacêutica, Universidade do Sul de Santa Catarina, 88704-900, Tubarão – SC – Brazil

## Abstract

In this study, implantable polycaprolactone/fluorouracil tablets were additively manufactured by selective laser sintering using different laser power levels. PCL/FU tablets showed on SEM-EDS small particles of fluorouracil dispersed on the surface and into the porous PCL matrix. The crystallinity values for the PCL/FU tablets were lower than for the pure PCL tablets, probably due to interaction of the FU particles with the polymer chains during the solidification process. The PCL/FU tablets prepared using the higher laser power (7 W) had the highest flexural modulus, probably due to better PCL particle coalescence, higher sinter degree and the dispersion of FU particles in the co-continuous porous PCL matrix. Initially the PCL/FU tablets provided a rapid release of a high concentration of the drug at the site of the cancer cells and a subsequent controlled release sustaining levels of the chemotherapeutic agent in the region of the tumor. This 2-stage release of the drug can be a desirable profile in cartilage cancer treatment.

## Introduction

Chondrosarcoma is a malignant cartilaginous tumor. It is the second largest group of primary bone tumors. Highest prevalence is found between the fourth and sixth decade, with an equal male to female ratio. Approximately 90% of chondrosarcoma are described as conventional type. They arise centrally in the metaphyseal region of long bones, but can also develop in flat bones such as pelvis, rib and scapula. A minority (up to 15%) of conventional chondrosarcoma develops from the surface of bone as a result of malignant transformation within the cartilage cap of a pre-existent osteochondroma and is therefore called secondary or peripheral chondrosarcoma [1]. For all grades of non-metastatic chondrosarcoma en-block resection offers the best recurrence free survival, surgical management is related to grade, type and site. Chemotherapy is possibly effective in mesenchymal chondrosarcoma, and of uncertain value in dedifferentiated chondrosarcoma [2,3]. There is an urgent need for new treatment options for bone cancer patients. Local drug delivery systems can be an option to the cartilage-bone cancer treatment.

Targeted drug delivery was first conceptualized in the early 1900s. Over the last 30 years, site-specific delivery of drugs has remained an elusive goal despite intensive research efforts by both academia and industry. Minimally invasive, intratumoral strategies for the treatment of solid tumors promise to substantially improve the therapeutic outcomes for many cancers. Systemic chemotherapy is often limited by severe toxicity and patient morbidity, and local cancer therapy can overcome this limitation by maximizing drug delivery to malignant tissues while minimizing systemic exposure to the chemotherapeutic drugs [4-6].

Polyanhydride/carmustine wafer (Gliadel®) is the only clinically approved chemotherapeutic implant by the Food and Drug

Administration (FDA) for the delivery of anticancer agents to a surgical cavity after primary surgical resection of malignant glioblastoma, an aggressive brain cancer. Combining minimally-invasive treatments with controlled release technology provides opportunities for treating cancers in a safe and effective manner by placing drug-loaded implants directly into solid tumors or in resection cavities. However, it is likely that future chemotherapeutic implants will be optimized for use in a variety of different tumors to maximize patient comfort and survival [7-9].

Additive Manufacturing, also known as 3D printing, offers the possibility to create three-dimensional structures from various materials and blends with less limitations in geometry compared to conventional manufacturing techniques. Selective Laser Sintering (SLS) is an Additive Manufacturing process that creates objects, layer by layer, using infrared laser beams to process powder materials [10-12]. The level of control over the microstructure of the SLS parts is dependent on the process parameters (laser power, scan speed and spot diameter of the laser beam, and bed temperature) and the powder properties. The particle shape and size distribution influence the powder packing density, while the melting flow behavior and the thermal stability define the laser power and scan speed [13-19]. In recent years, the SLS process has shown great prominence in the medical field, such as in the manufacturing of drug delivery devices (DDD) [14-19].

**Correspondence to:** Salmoria GV, NIMMA, Department of Mechanical Engineering, Federal University of Santa Catarina, 88040-900 Florianópolis, SC, Brazil, E-mail: gean.salmoria@ufsc.br

**Key words:** polycaprolactone/fluorouracil, implantable drug delivery, cartilage cancer treatment, selective laser sintering

**Received:** May 29, 2017; **Accepted:** June 24, 2017; **Published:** June 26, 2017

Polycaprolactone (PCL) is a biodegradable polyester approved by FDA for use in the human body as a drug delivery device. The particle size and shape along with the laser power are used to design and control the porosity of the polycaprolactone matrix and, consequently, control the drug release from DDDs [15-19].

Fluorouracil (5Fluoro1H, 3Hpyrimidine2,4dione) acts as a thymidylate synthase (TS) inhibitor, interrupting the action of this enzyme blocks the synthesis of pyrimidine thymidine, which is a nucleoside required for DNA replication. The TS enzyme methylates deoxyuridine monophosphate to form thymidine monophosphate (dTMP). Administration of fluorouracil (FU) causes an insufficiency in dTMP due to the formation of the FUTS complex, resulting in high cytotoxicity and death of cancerous cells via thymineless [20-22]. In this study, polycaprolactone/fluorouracil tablets were produced by selective laser sintering using different laser energy densities. The structure, mechanical properties and drug release of the tablets were evaluated and correlated with the processing conditions.

## Experimental

### Materials

The polymeric powder used in this study was commercial polycaprolactone (PCL; Sigma-Aldrich Company) with an average molecular weight of 70,000 to 90,000 g/mol, glass transition temperature (T<sub>g</sub>) of -60 °C, melting temperature (T<sub>m</sub>) of 60 °C, melt flow index of 1.00 g/10 min, and density of 1.145 g/cm<sup>3</sup> at 25 °C. The PCL was ground cryogenically in a mechanical grinder and sieved. The particle sizes obtained were from 125 to 212 μm. The fluorouracil (FU) was manufactured by Hubei Gedian Pharmaceutical Co.. The melting temperature of fluorouracil is 282 °C. The blend powder was prepared by a mechanical mixing in a Y-type rotator for 10 minutes at 30 rpm.

### Tablets manufactured by selective laser sintering

The pure PCL and PCL/FU tablets, with dimensions of around 35×5×1.4 mm, were sintered in a selective laser sintering system with a 9 W power CO<sub>2</sub> laser and laser beam diameter of 250 μm. This study was performed in the open air and the powder bed temperature was 45 °C. The laser scanning speed was maintained at 350 mm/s. The building layer thickness used was 250 μm and the spacing between the laser scans was 125 μm. The laser power used to produce the tablets is shown in Table 1.

### Infrared and near-infrared spectroscopy

The infrared spectra of the polymers were obtained using a Perkin-Elmer Frontier MIR/NIR spectrophotometer in the attenuated total reflectance (ATR) mode, performing 20 scans at a resolution of 4 cm<sup>-1</sup>, in order to characterize the absorbance peaks of the polymers and blends. Near infrared spectra of the polymers and blends were obtained performing 20 scans, using a NIR Analyzer in reflectance mode from 1000–2500 nm.

### Scanning electron microscopy and differential scanning calorimetry

The morphology of the tablets were examined by scanning electron microscopy (SEM), using an XL 30 Phillips microscope. The specimens were coated with gold in a Bal-Tec Sputter Coater SCD005.

Differential scanning calorimetry (DSC) curves were obtained using a differential scanning calorimeter (Perkin Elmer) from 0 to 300 °C at a heating rate of 10 °C/min. The average sample size was 5 mg and the nitrogen flow-rate was 25 cm<sup>3</sup>/min.

**Table 1.** Pure PCL and PCL/FU tablets manufactured with different power.

Tablet	Fluorouracil content (%)	Laser power (W)
PCL	0	3.0
PCL	0	7.0
PCL/FU	10	3.0
PCL/FU	10	7.0

### Mechanic tests

The DMA Q800 system of TA instruments with a single cantilever clamp was used for the mechanical tests of the SLS manufactured tablets (dimensions 35×5×1.4 mm). A ramp of 2N/min from 0 to 18N was applied for the quasi-static flexural tests. The fatigue test was performed applying an oscillatory deformation. The amplitude used was 750 μm in both directions, under a frequency of 1 Hz, at 37 °C.

### Drug release and recovery of incorporated fluorouracil

The dry specimens with known drug content and thickness were immersed in a 50-mL phosphate buffer solution (pH:7.4) (to maintain sink conditions), shaken horizontally in a Dubnoff bath (Quimis S.A, Brazil) at a rate of 60 rev/min to minimize the boundary effect, and maintained at a temperature of 37.0±0.5 °C. The whole volume of the receptor solution was removed periodically and replaced with fresh a solution. After suitable dilution with the buffer solution, the total drug release was obtained against a predetermined calibration curve (five dilutions between 0.0020 and 0.0220 mg/mL) using a UV-Vis spectrophotometry at λ<sub>max</sub> of 265 nm, on a Hitachi 2010 double-beam UV-visible spectrophotometer.

In order to carry out the recovery test, tablet segments obtained from three different portions of the total material produced under each condition were collected. Each piece was weighed and cut into smaller pieces to increase the surface area in contact with the solvent added (10 mL of methanol; in triplicate). Samples were kept in an ultrasonic bath for 2 h and then analyzed by UV-vis spectrophotometry, at λ<sub>max</sub> of 265 nm, on a Hitachi 2010 double-beam UV-visible spectrophotometer.

## Results and discussion

The micrographs of the pure PCL and PCL/FU tablet surfaces manufactured with different laser power are shown in Figures 1A-D. The tablets presented uniform morphology, coalescence of particles and interconnected pores distributed in the PCL matrix, properties which are of great interest for application in implantable drug delivery.

The PCL/FU tablets manufactured by selective laser sintering presented an extensive neck formation between the particles and co-continuous phases, particularly for structures formed using the higher laser energy (Figure 1D). On the other hand, the pure PCL tablets produced with the lower laser energy showed a low degree of sintering with the formation of small necks between the particles (Figure 1A). The PCL/FU tablets have a greater particle coalescence probably due to the greater laser absorption by the fluorouracil particles.

Figure 2 shows the micrographs of the PCL/FU tablets with the EDS nitrogen atom contrast and nitrogen chart. The EDS Nitrogen contrast for the PCL/FU tablets shows the presence of small particles of fluorouracil distributed throughout the polycaprolactone matrix. The EDS analysis revealed the proportion of carbon, oxygen, nitrogen and fluorine atoms present in the PCL matrix and in the FU particle composition (Figure 2E) and confirmed the presence of fluorouracil dispersed throughout the porous PCL matrix.

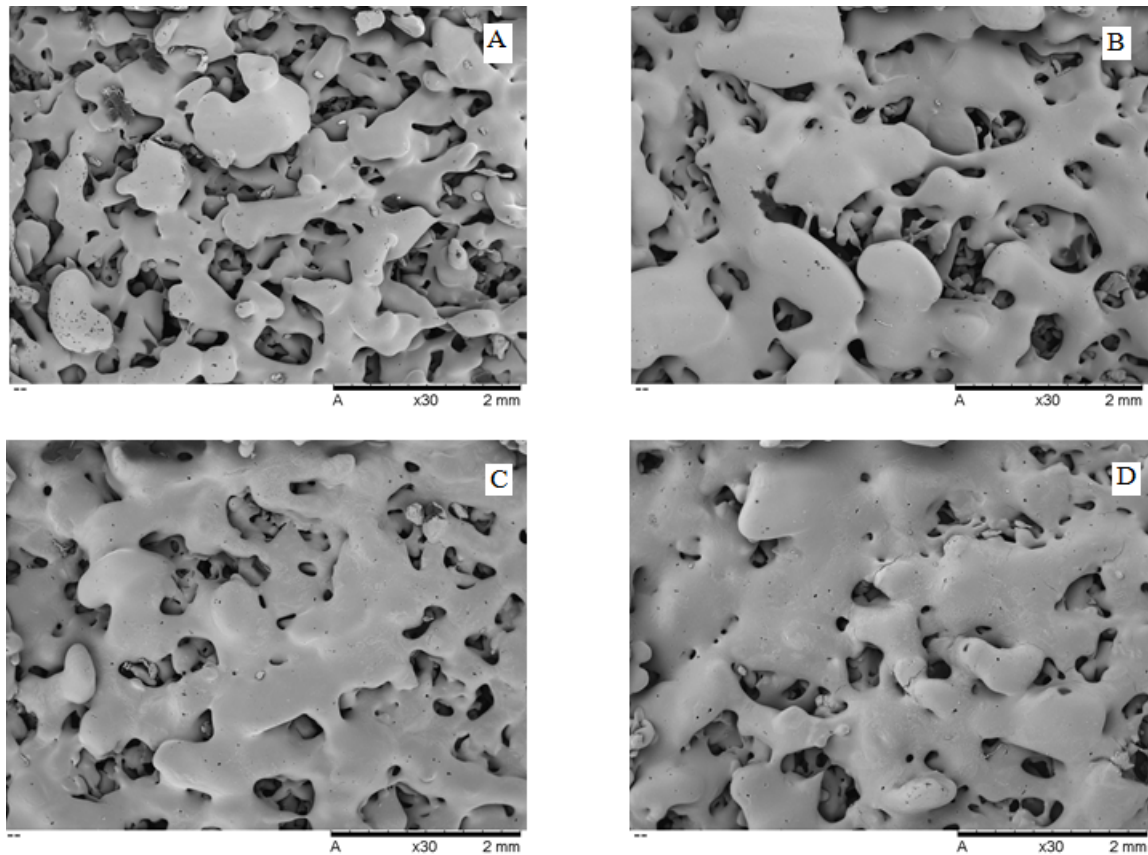


**Figure 1.** Surface micrographs of pure PCL and PCL/FU tablets sintered using different power conditions: PCL 3W (A), PCL 7W (B), PCL/FU 3W (C), and PCL/FU 7W (D).

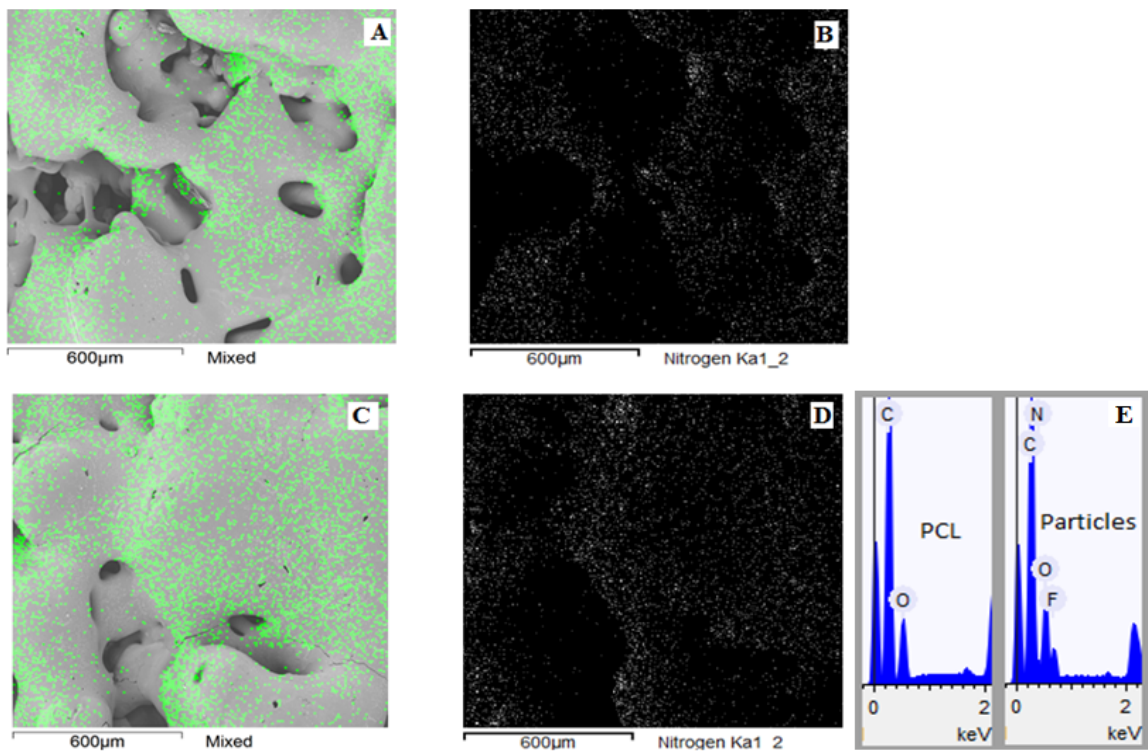


**Figure 2.** Surface micrographs presenting the EDS Nitrogen contrast and chart of PCL/FU tablets sintered using different power conditions: PCL/FU 3W (A and B), PCL/FU 7W (C and D), and the EDS composition of PCL matrix and FU particles in the tablet (E).

Figure 3 shows the FTIR spectra for the fluorouracil (A), pure PCL (B and C) and PCL/FU tablets (D and E) prepared using different laser power. The band present in the fluorouracil spectrum in the 3100–3000  $\text{cm}^{-1}$  region represents =C–H stretching. The absorption peaks at about 2938  $\text{cm}^{-1}$  and 2831  $\text{cm}^{-1}$  are attributed to the –CH<sub>2</sub> group. The fluorouracil shows bands in the 1580–1650  $\text{cm}^{-1}$  region corresponding to the stretching of C=N and C=C bonds in the ring [23]. The absorption peak at about 1724  $\text{cm}^{-1}$  is due to the stretching vibration of the C=O bond. The bands at about 1450  $\text{cm}^{-1}$  and 1350  $\text{cm}^{-1}$  are attributed to substituted pyrimidine compounds. The absorption peaks at 1180  $\text{cm}^{-1}$  and 1251  $\text{cm}^{-1}$  are assigned to the C–O and C–N bond frequencies, respectively [23]. The absorption peak at about 1230  $\text{cm}^{-1}$  is due to the fluorine bond on the ring. Absorption bands are also observed in the 820–550  $\text{cm}^{-1}$  region, which are attributed to the C–F deformations [23]. The pure PCL tablets (Figure 3B and C) show peaks at 2940, 2863, 1721, 1294, 1164, 1157 and 717  $\text{cm}^{-1}$  related to the CH<sub>2</sub> asymmetric stretching, CH<sub>2</sub> symmetric stretching, C=O carbonyl stretching, C–O stretching in the crystalline phase, asymmetric C–O–C stretching, C–O stretching in the amorphous phase and CH<sub>2</sub> rocking, respectively (Figure 5B) [24, 25].

The main peaks in the FTIR spectra for the PCL/FU tablets (Figure 3D and E) were the same as those observed in the spectra for the pure PCL tablets. The existence of a shoulder band in the 1580–1650  $\text{cm}^{-1}$  region and the peaks around 600  $\text{cm}^{-1}$  are related to the C=C and C=N ring bonds and the C–F bond in the fluorouracil structure, verifying the presence of the drug. The intermolecular interaction was evaluated from the peaks related to PCL, the main component (90 wt%). The C=O stretching peak of PCL (1721  $\text{cm}^{-1}$ ) and the other peaks presented no dislocations, suggesting that there are no intermolecular interactions between FU and PCL.

The full near-infrared (NIR) spectrum extends from 700 nm to 2500 nm (14285 to 4000  $\text{cm}^{-1}$ ). NIR spectra are divided into three distinct spectral windows. Absorption features in the NIR range from 800 to 1200 nm correspond to higher order overtones and combinations associated with the CH, NH, and OH bonds. Information in the first overtone range from 1500 to 1900 nm originates from the first overtone of stretching vibrations of the CH and OH groups. The chemical information within the combination range from 2000 to 2500 nm corresponds to the combination of bending and stretching vibrations associated with the CH, NH, and OH molecular groups [26,27]. The NIR spectrum of pure fluorouracil over this spectral range is presented in Figure 4, A. This spectrum reveals a broad absorption band centered at 2200 nm related to the urea group and the ring structure. This region of the NIR spectrum is dominated by the second-overtone carbonyl stretching bands and the N–H combination bands. This later band corresponds to the combination of the symmetric and asymmetric N–H stretching coupled with the N–H bending vibration. Systems containing aryl rings also showed absorption in the 2130 to 2160 nm region [26]. The first overtones of the asymmetric and symmetric N–H stretches for fluorouracil are buried under the 1700 nm [28]. The NIR spectra of pure Polycaprolactone tablets (Figure 4B and C) show a small peak at 1200 nm related to the second-overtone of C–H bonds in the methylene groups, and an intense band at 1670–1780 nm relative to the first overtone of C–H. The 1900 nm and 1950 nm regions show the second-overtone carbonyl stretching and third C–O overtone bands, respectively. The combination bands from the C–H bonds in the methylene groups are present from 2250 to 2300 nm [29]. The NIR spectra of PCL/FU tablets presented (Figure 4D and E) the same bands as pure PCL, the major component, with an additional peak at 2330 nm relative to the presence of fluorouracil at 10 %.

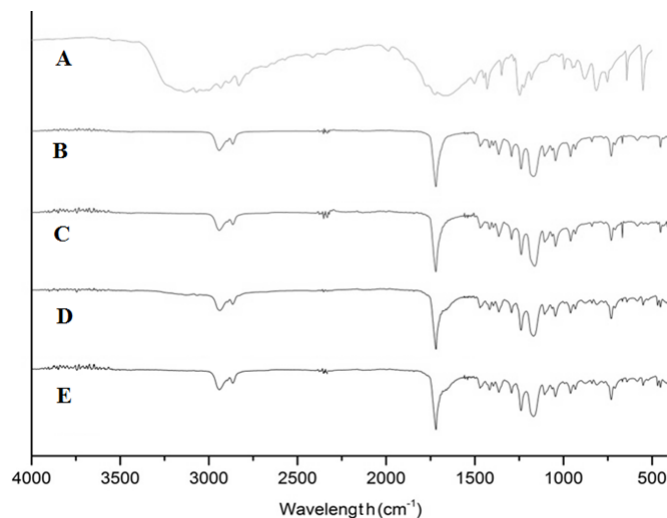


**Figure 3.** FTIR-ATR spectra for fluorouracil (A), pure PCL and PCL/FU tablets sintered using different power conditions: PCL 3W (B), PCL 7W (C), PCL/FU 3W (D), and PCL/FU 7W (E).

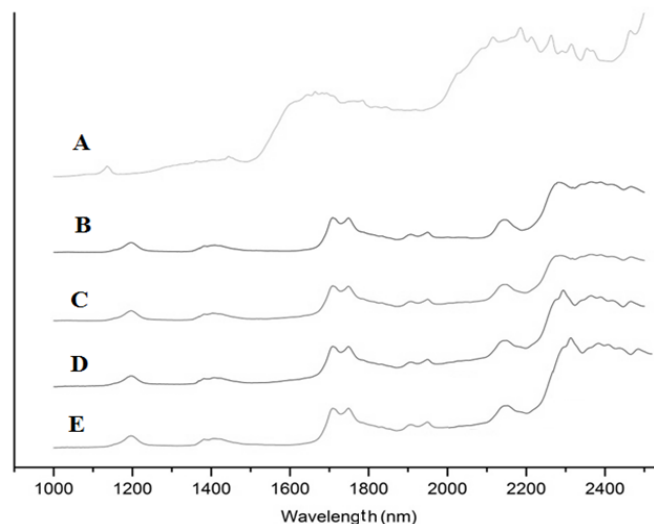


**Figure 4.** Near-FTIR spectra for fluorouracil (A), pure PCL and PCL/FU tablets sintered using different power conditions: PCL 3W (B), PCL 7W (C), PCL/FU 3W (D), and PCL/FU 7W (E).

The DSC Thermograms for pure fluorouracil, PCL and PCL/FU tablets in Figure 5 show the PCL and fluorouracil melting peaks at 60 and 284 °C, respectively. Melting temperature and crystallinity values for the PCL and PCL/FU tablets are shown in Table 2. There was no significant variation in the melting temperature among all the tablets, but the crystallinity values for the PCL/FU tablets were slightly lower than that for the pure PCL sintered using the same conditions. This difference is probably due to interaction of the drug particles with the polymer chains during the solidification process. The occurrence of this phenomenon suggests the existence of a low chemical affinity among the components at the molecular level. Higher laser energy seems to cause a small decrease in the crystallinity of the PCL and PCL/FU tablets, probably due to the faster cooling rate.

Figure 6 shows the flexion test curves for PCL and PCL/FU tablets are presented in. Table 3 shows the values for the flexural modulus and strength at 5% of elongation for the pure PCL and PCL/FU tablets. The pure PCL tablets manufactured with low laser energy (A) showed a

**Table 2.** Melting enthalpy, melting temperature and DSC crystallinity of pure PCL and PCL/FU tablets prepared with different laser sintering power.

Specimen	$\Delta H_{PCL}$ (J/g)	Tm (°C)	PCL Crystallinity (%)	$\Delta H_{FU}$ (J/g)	Tm (°C)	FU content (%)
Pure FU	-	-	-	237 ± 6.2	284.1 ± 0.3	100
PCL 3W	79.7 ± 1.2	60.7 ± 0.3	56.1 ± 1.1	-	-	-
PCL 7W	78.5 ± 1.4	60.5 ± 0.3	55.3 ± 1.3	-	-	-
PCL/FU 3W	69.3 ± 1.4	60.4 ± 0.4	53.7 ± 1.3	22.7 ± 3.1	283.7 ± 0.4	10 ± 1
PCL/FU 7W	68.1 ± 1.1	60.1 ± 0.3	53.2 ± 1.0	23.1 ± 3.2	283.8 ± 0.3	11 ± 1

\*Crystallinity values based in the enthalpy of melting of 100% crystalline PCL, 142.0 J/g [30]. For the PCL/FU tablets, only 90 % of the weight was considered in the PCL crystallinity calculus, since 10 % was FU.

**Table 3.** Flexural modulus and strength of pure PCL and PCL/FU tablets prepared with different laser sintering power.

Specimen	Flexural Modulus (MPa)	Strength at 5% strain (MPa)
PCL 3W	12.3 ± 2.6	1.1 ± 0.2
PCL 7W	13.6 ± 1.5	1.7 ± 0.3
PCL/FU 3W	14.2 ± 2.3	1.7 ± 0.4
PCL/FU 7W	19.9 ± 2.4	2.9 ± 0.4

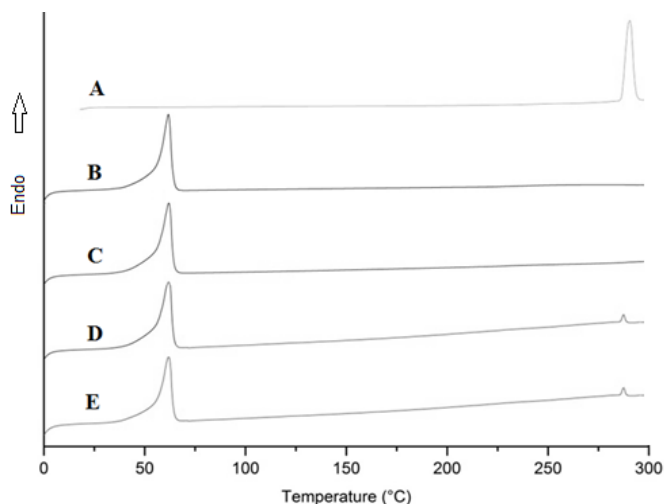


**Figure 5.** DSC thermograms for pure fluorouracil (A), PCL 3W (B), PCL 7 (C), PCL/FU 3W (D) and PCL/FU 7W (E).

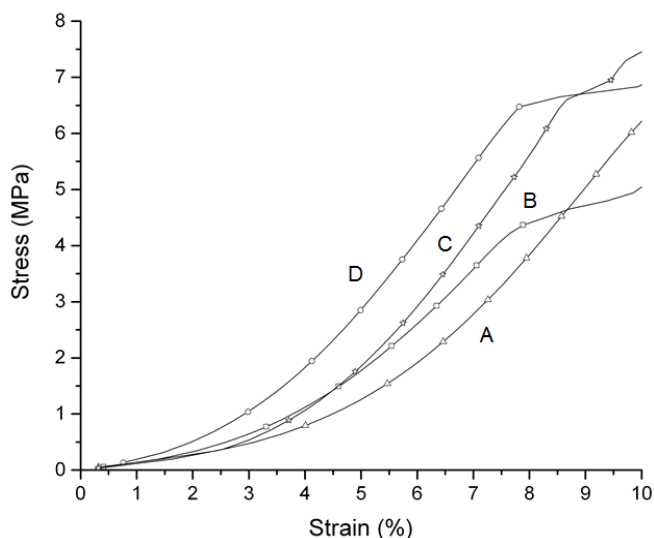


**Figure 6.** Flexural test curves of pure PCL and PCL/FU tablets sintered using different power conditions: PCL 3W (A), PCL 7W (B), PCL/FU 3W (C), and PCL/FU 7W (D).

lower value for flexural modulus (12.3 MPa) than the PCL/FU tablets. The PCL/FU tablets manufactured with high laser energy (D) showed a higher value for the flexural modulus (19.9 MPa) than the PCL/FU tablets prepared with 3W of laser power. These results demonstrated that the stiffness of the PCL tablets increases with the use of higher laser energy, providing higher polymer flow, greater contact between the particles and greater neck formation. The flexural modulus of PCL tablets increases with the presence of fluorouracil probably due to a hardening effect caused by its particles within the PCL matrix.

The fatigue curves for pure PCL and PCL/FU tablets are shown in Figure 7. These curves show the stress resistance as a function of the cycle number. The pure PCL tablets prepared using both the low and high laser energy (A and B, respectively) showed higher fatigue strength than the PCL/FU tablets, and smaller stress variations. The fatigue curve for the PCL/FU tablets show higher stress variations up to 1000 cycles, probably due to the hardening effect of the fluorouracil particles that cause a loss of flexibility.

Figure 8 shows the drug release profiles of PCL/FU tablets. The results showed that both tablets manufactured using low and high laser power had an initial rapid drug release. The PCL/FU tablets showed a burst of drug release with values of around 83 mg/g cumulative drug released. This may be attributed to the aqueous solubility of FU (12.5 mg/ml) leading to a rapid dissolution of the drug molecules present in the porous PCL matrix. After this initial burst in the first hour, the release rate became slower and stabilized after 5 hours for both types of PCL/FU tablets (A and B). The % FU released after 48 hours from both tablets types was nearly 97%. The total amount of drug released was similar for PCL/FU tablets manufactured using the lower and higher laser powers and are associated with small differences presented by both condition in the sintering degree and porosity. This drug release pattern is very common with FU polymeric drug delivery systems and has been reported by many researchers [31-33]. The initial amount of FU released by the sintered PCL/FU tablets is a desirable profile to provide a high initial concentration of the drug locally in the cancer cells following implantation. The slow and controlled release of the drug subsequently will allow for sustained levels of the chemotherapeutic agent at the cancer site [34,35]. This may be beneficial therapeutically since FU molecules and small particulates are capable of preferentially accumulating within tumors via the delivery of the implanted tablet.

**Conclusions**

This work has demonstrated that the additive manufacturing of PCL/FU tablets is possible, and it can be done by selective laser sintering with efficiency. PCL/FU tablets were seen on SEM-EDS as small particles of fluorouracil dispersed over the surface and throughout the porous PCL matrix. The main peaks in the FTIR and NIR spectra for the PCL/FU tablets were the same as those observed in the spectra for the pure PCL tablets. The existence of peaks at 600 cm<sup>-1</sup>

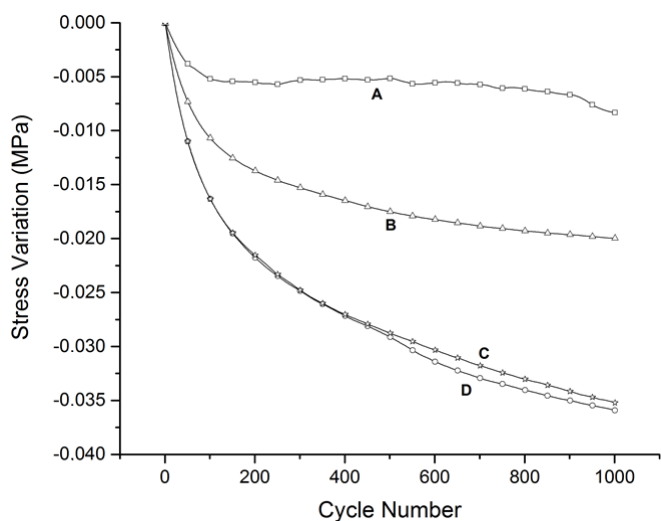


**Figure 7.** Fatigue test curves of pure PCL and PCL/FU tablets sintered using different power conditions: PCL 3W (A), PCL 7W (B), PCL/FU 3W (C), and PCL/FU 7W (D).

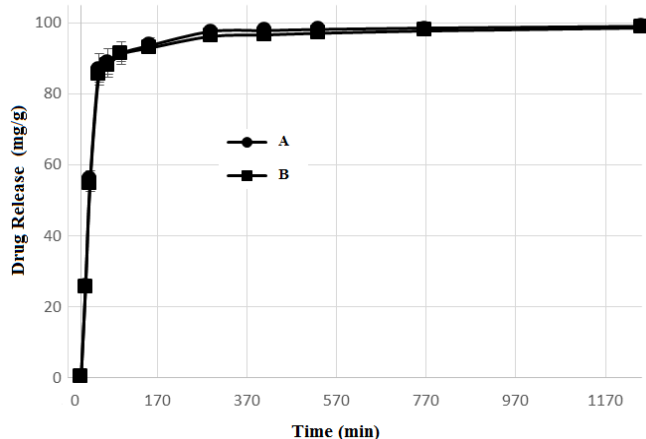


**Figure 8.** Fluorouracil release as a function of time for PCL/FU tablets manufactured using 3W (A) and 7W (B) of laser power.

related to the C-F bond, and an additional peak at 2330 nm relative to the fluorouracil structure, confirm its presence at 10 % content by both techniques. The crystallinity values for the PCL/FU tablets were lower than that for the pure PCL tablets, which is probably due to interaction of the FU particles with the polymer chains during the solidification process. The PCL/FU tablets prepared using the higher laser power (7 W) had the highest flexural modulus, probably due to better coalescence of the PCL particles, higher sinter degree and the dispersion of FU particles in the co-continuous porous PCL matrix. The PCL/FU tablets initially showed a rapid drug released due to the hydrophilic character of fluorouracil. A high initial concentration of the drug locally in the cancer cells following implantation is a desirable profile. The slow and controlled release of the drug presented subsequently by PCL/FU tablets is interesting for sustained levels of the chemotherapeutic agent in the region of the tumor with potential improvement for cartilage cancer treatments.

### Acknowledgement

The authors would like to thank PRONEX/FAPESC, CNPQ and FINEP for financial support and Mr. Paulo C.M. Rosa for the inspiration.

### References

- Bertoni F, Bacchini P (1998) Classification of bone tumors. *Eur J Radiol* 27 Suppl 1: S74-76. [Crossref]
- Dickey ID, Rose PS, Fuchs B, Wold LE, Okuno SH, et al. (2004) Dedifferentiated chondrosarcoma: the role of chemotherapy with updated outcomes. *J Bone Joint Surg Am* 86-86A: 2412-8. [Crossref]
- Gelderblom H, Hogendoorn PC, Dijkstra SD, van Rijswijk CS, Krol AD, et al. (2008) The clinical approach towards chondrosarcoma. *Oncologist* 13: 320-329. [Crossref]
- Olivi A, Ewend MG, Utsuki T, Tyler B, Domb AJ, et al. (1996) Interstitial delivery of carboplatin via biodegradable Polymers is effective against experimental glioma in the rat. *Cancer ChemotherPharmacol* 39: 90-96. [Crossref]
- Qian F, Saidel GM, Sutton DM, Exner A, Gao J (2002) Combined modeling and experimental approach for the development of dual-release polymer millirods. *J Control Release* 83: 427-435. [Crossref]
- Tacara O, Sriamornsak P, Dassa CR (2013) Doxorubicin: an update on anticancer molecular action, toxicity and novel drug delivery systems. *J Pharm Pharmacol* 65: 157-170. [Crossref]
- Weinberg BD, Ai H, Blanco E, Anderson JM, Gao J (2007) Antitumor efficacy and local distribution of doxorubicin via intratumoral delivery from polymer millirods. *J Biomed Mater Res A* 81: 161-170. [Crossref]
- Weinberg BD, Blanco E, Gao J (2008) Polymer Implants for Intratumoral Drug Delivery and Cancer Therapy. *J Pharm Sci* 97: 1681-1702. [Crossref]
- Solorio L, Patel RB, Wu H, Krupka T, Exner AA (2010) Advances in image-guided intratumoral drug delivery techniques. *TherDeliv* 1: 307-322. [Crossref]
- Low KH, Leong KF, Chua CK, Du ZH, Cheach CM (2001) Characterization of SLS parts for drug delivery devices. *Rapid Prototyping Journal* 7: 262-267.
- Leong KF, Phua KKS, Chua CK, Du ZH, Teo KOM (2001) Fabrication of Porous Polymeric Matrix Drug Delivery Devices Using the Selective Laser Sintering Technique. *Proc Inst Mech Eng H* 215: 191-201. [Crossref]
- Cheah CM, Leong KF, Chua CK, Low KH, Quek HS (2002) Characterization of microfeatures in selective laser sintered drug delivery devices. *Proc Inst Mech Eng H* 216: 369-383. [Crossref]
- Yeong WY, Chua CK, Leong KF, Chandrasekaran M (2004) Rapid Prototyping in Tissue Engineering: Challenges and Potential. *Trends Biotechnol* 22: 643-652. [Crossref]
- Leong KF, Chua CK, Gui WS, Verani WSG (2006) Building Porous Biopolymeric Microstructures for Controlled Drug Delivery Devices Using Selective Laser Sintering. *The International Journal of Advanced Manufacturing Technology* 31: 483-489.
- Leong KF, Wiria FE, Chua CK, Li SH (2007) Characterization of a poly-epsilon-caprolactone polymeric drug delivery device built by selective laser sintering. *Biomed Mater Eng* 17: 147-157. [Crossref]
- Salmoria GV, Klauss P, Zepon K, Kanis LA, Roesler CRM, et al. (2012) Development of functionally-graded reservoir of PCL/PG by selective laser sintering for drug delivery devices. *Virtual and Physical Prototyping* 7: 107-115.
- Salmoria GV, Klauss P, Zepon KM, Kanis LA (2013) The effects of laser energy density and particle size in the selective laser sintering of polycaprolactone/progesterone specimens: morphology and drug release. *International Journal of Advanced Manufacturing Technology* 66: 1113-1118.
- Salmoria GV, Hotza D, Klauss P, Kanis LA, Roesler CRM (2014) Manufacturing of Porous Polycaprolactone Prepared with Different Particle Sizes and Infrared Laser Sintering Conditions: Microstructure and Mechanical Properties. *Advances in Mechanical Engineering* 640496.
- Salmoria GV, Cardenuto MR, Roesler CRM, Zepon KM, Kanis LA (2016) PCL/Ibuprofen Implants Fabricated by Selective Laser Sintering for Orbital Repair. *Procedia CIRP* 49: 188-192.
- Hiroshi Seno, Kazuki Ito, Koichi Kojima, Nobuaki Nakajima, Tsutomu Chiba (1999) Efficacy of an implanted drug delivery system for advanced hepatocellular carcinoma using 5-fluorouracil, epirubicin and mitomycin C. *Journal of Gastroenterology and Hepatology*. 14: 811-816.
- Wang S, Chen H, Cai Q, Bei J (2001) Degradation and 5-Fluorouracil Release Behavior in vitro of Polycaprolactone/poly(ethylene oxide)/polylactide Tri-component Copolymer. *Polym Advm Technol* 12: 253-258.

22. Martini LG, Collett JH, Attwood D (2000) The release of 5-fluorouracil from microspheres of poly(epsilon-caprolactone-co-ethylene oxide). *Drug Dev Ind Pharm* 26: 7-12. [Crossref]
23. Singh P, Tyagi G, Mehrotra R, Bakhshi AK (2009) Thermal stability studies of 5-fluorouracil using diffuse reflectance infrared spectroscopy. *Drug Test Anal* 1: 240-244. [Crossref]
24. Pant HR, Neupane MP, Pant B, Panthi G, Oh H, et al. (2011) Fabrication of highly porous poly(e-caprolactone) fibers for novel tissue scaffold via water-bath electrospinning. *Colloids Surf B Biointerfaces* 88: 587-592. [Crossref]
25. Paquet O, Krouit M, Bras J, Thilemans W, Belgacem M (2010) Surface modification of cellulose by PCL grafts. *Acta Materialia* 58: 792-801.
26. Edward SK, Mahpour M (1973) The identification and origin of N-H overtone and combination bands in the near-infrared spectra of simple primary and secondary amides. *Spectrochim Acta A* 29:1233-1246.
27. Hazen KH, Arnold MA, Small GW (1998) Measurement of glucose in water with first-overtone near-infrared spectra. *Appl Spectrosc* 52: 1597-1605.
28. Eddy CV, Arnold MA (2001) Near-Infrared Spectroscopy for Measuring Urea in Hemodialysis Fluids. *ClinChem* 47: 1279-1286. [Crossref]
29. Crandall EW, Jagtap AN (1977) The near-infrared spectra of polymers. *J Appl Polym Sci* 21: 449-454.
30. Crescenzi V, Manzini G, Galzolari G, Borri C (1972) Thermodynamics of fusion of poly-beta-propiolactone and poly-e-caprolactone. Comparative analysis of the melting of aliphatic polylactone and polyester chains". *Eur Polym J* 8: 449-463.
31. Yassin AEB, Anwer MK, Mowafy HA, El-Bagory IM, Bayomi MA, et al. (2010) Optimization of 5-fluorouracil solid-lipid nanoparticles: a preliminary study to treat colon cancer. *Int J Med Sci* 7: 398-408. [Crossref]
32. Lee JS, Chae GS, An TK, Khang G, Cho SH, et al. (2003) Preparation of 5-fluorouracil-loaded poly(L-lactide-co-glycolide) wafer and evaluation of in vitro release behavior. *Macromolecular Research* 11: 183-188.
33. Hanafy AFAH, El-Egaky AM, Mortada SAM, Molokhia AM (2009) Development of implants for sustained release of 5-fluorouracil using low molecular weight biodegradable polymers. *Drug Discov Ther* 3: 287-295. [Crossref]
34. Sairam M, Babu VR, Naidu BVK, Aminabhavi TM (2006) Encapsulation efficiency and controlled release characteristics of crosslinked polyacrylamide particles. *Int J Pharm* 320: 131-136. [Crossref]
35. Gao H, Gu Y, Ping Q (2007) The implantable 5-fluorouracil-loaded poly(L-lactic acid) fibers prepared by wet-spinning from suspension. *J Control Release* 118: 325-332. [Crossref]